Quasiuniversal Properties of Neutron Star Mergers

Sebastiano Bernuzzi,[1] Alessandro Nagar,[2] Simone Balmelli,[3] Tim Dietrich,[1] and Maximiliano Ujevic[4]
[1]Theoretical Physics Institute, University of Jena, 07743 Jena, Germany
[2]Institut des Hautes Etudes Scientifiques, 91440 Bures-sur-Yvette, France
[3]Physik-Institut, Universität Zürich, 8057 Zürich, Switzerland
[4]Centro de Ciências Naturais e Humanas, Universidade Federal do ABC, 09210-170, Santo André, São Paulo, Brazil
(Received 26 February 2014; published 20 May 2014)

Binary neutron star mergers are studied using nonlinear $3+1$ numerical relativity simulations and the analytical effective-one-body model. The effective-one-body model predicts quasiuniversal relations between the mass-rescaled gravitational wave frequency and the binding energy at the moment of merger and certain dimensionless binary tidal coupling constants depending on the stars' Love numbers, compactnesses, and the binary mass ratio. These relations are quasiuniversal in the sense that, for a given value of the tidal coupling constant, they depend significantly neither on the equation of state nor on the mass ratio, though they do depend on stars spins. The spin dependence is approximately linear for small spins aligned with the orbital angular momentum. The quasiuniversality is a property of the conservative dynamics; nontrivial relations emerge as the binary interaction becomes tidally dominated. This analytical prediction is qualitatively consistent with new, multiorbit numerical relativity results for the relevant case of equal-mass irrotational binaries. Universal relations are, thus, expected to characterize neutron star mergers dynamics. In the context of gravitational wave astronomy, these universal relations may be used to constrain the neutron star equation of state using waveforms that model the merger accurately.

DOI: 10.1103/PhysRevLett.112.201101 PACS numbers: 04.25.D-, 04.30.Db, 95.30.Sf, 97.60.Jd

Introduction.—Binary neutron star (BNS) inspirals are among the most promising sources for the advanced configurations of the ground-based gravitational wave (GW) detector network [1]. Advanced configurations of LIGO and Virgo detectors are expected to listen to ~ 0.4–$400\ \mathrm{yr}^{-1}$ events starting from 2016–2019 [2]. Direct GW observations will then probe such systems in the near future. In particular, because the late-inspiral-merger phase depends crucially on the stars' internal structure, the measurement of the tidal polarizability parameters from GWs will put the strongest constraints on the unknown nuclear equation of state (EOS) [3–6].

An accurate modeling of neutron star mergers requires numerical relativity (NR). In recent years, simulations have become fairly robust, but exploring the physical parameter space remains a challenge out of reach. Furthermore, the interpretation of simulation data can be nontrivial: meaningful quantities must be gauge invariant and possibly have well-defined post-Newtonian (PN) limits. The GW phasing analysis for multiorbits (~ 10) simulations was performed by some groups, e.g., [7–9]. The BNS dynamics, expressed via the gauge-invariant relation between binding energy and angular momentum [10,11], was recently analyzed in both the nonspinning and spinning case [12,13]. For both observables a solid analytical framework, although approximate, is essential for extracting information from the simulations.

Despite these detailed studies, simple, fundamental questions about the merger physics still lack quantitative answers. For instance, a test mass in the Schwarzschild metric of mass M has a last stable orbit (LSO) at $R_{\mathrm{LSO}} = 6M$, (we use units with $G = c = 1$) with dimensionless (or mass-reduced) orbital frequency $M\Omega_{\mathrm{LSO}}^{\mathrm{Schw}} = 6^{-3/2} \approx 0.06804$. The associated GW frequency $2M\Omega_{\mathrm{LSO}}^{\mathrm{Schw}} \approx 0.13608$ is commonly used to mark the end of the quasiadiabatic BNS inspiral, setting M equal to the total mass of the binary. Similarly, the specific LSO binding energy $E_{b\,\mathrm{LSO}}^{\mathrm{Schw}} = (8/9)^{1/2} - 1 \approx -0.0572$ is used to estimate the total amount of GW energy emitted during the coalescence process. These numbers appear ubiquitously in BNS-related studies, e.g., Ref. [6], but are, in principle, no more than order of magnitude estimates as they neglect both finite mass ratio and finite size effects. Some questions arise: How to model or include these effects? How does the merger frequency and binding energy depend on the main parameters of the binary (EOS, mass ratio, and individual spins)? How accurate are the Schwarzschild LSO estimates? In this work, we use new multiorbit NR data and the analytical effective-one-body (EOB) approach problem to put forward some answers. We find that the GW frequency and binding energy at the moment of merger are characterized only by certain dimensionless tidal coupling constants (a fact also empirically observed in Ref. [5] for the frequency) and the stars spins as a consequence of a fundamental property of the underlying conservative dynamics.

EOB and the LSO.—The EOB formalism [14–17] maps the relativistic 2-body problem, with masses M_A and M_B, into the motion of an effective particle of mass

$\mu = M_A M_B/M$, with $M = M_A + M_B$, moving into an effective metric. It employs standard PN results (e.g., Ref. [18]) in a *resummed* form, and it is robust and predictive also in the strong-field and fast-motion regime. The EOB model can be completed with NR information; complete (inspiral-merger-ringdown) binary black hole waveforms for GW astronomy can be produced for general mass-ratio and spin configurations [11,19]. Tidal effects can also be included in the model [4,20]. The EOB model consists of three building blocks: (i) a Hamiltonian $H_{\rm EOB}$; (ii) a factorized gravitational waveform; and (iii) a radiation reaction force $\mathcal{F}_\varphi$. The EOB Hamiltonian is $H_{\rm EOB} = M\sqrt{1 + 2\nu(\hat{H}_{\rm eff} - 1)}$ where, in the nonspinning case, $\hat{H}_{\rm eff}(u, p_{r_*}, p_\varphi) \equiv H_{\rm eff}/\mu = \{A(u;\nu)[1 + p_\varphi^2 u^2 + 2\nu(4 - 3\nu)u^2 p_{r*}^4] + p_{r*}^2\}^{1/2}$, with $\nu \equiv \mu/M$, $u \equiv 1/r \equiv GM/Rc^2$, and $p_\varphi \equiv P_\varphi/(M\mu)$ is the dimensionless orbital angular momentum and $p_{r_*} \equiv \sqrt{A/B}\,p_r = P_r/\mu$ is a dimensionless radial momentum; $A(u;\nu)$ and $B(u;\nu)$ are the EOB potentials. The conservative dynamics ($\mathcal{F}_\varphi = 0$) along circular orbits ($p_{r_*} = 0$) is determined only by $A(u;\nu)$. Finite-size effects are formally 5PN. They are included in $A(u;\nu)$ by adding a tidal term $A^T(u;\nu)$ to the point-mass $A^0(u;\nu)$ contribution, i.e., $A(u) \equiv A^0(u;\nu) + A^T(u;\nu)$ [20]. The $A^0(u)$ function is analytically known at 4PN accuracy and formally reads $A^0_{\rm 4PN}(u;\nu) = 1 - 2u + \nu\hat{a}_{\rm 4PN}(u;\nu)$, where $\hat{a}_{\rm 4PN}(u;\nu) \equiv a_3 u^3 + a_4 u^4 + [a_5^c(\nu) + a_5^{\ln}\ln u]u^5$ [21]. We use here *only* the 4PN-accurate analytical information, and we do not add any "flexibility parameter" calibrated to NR data. The Taylor-expanded function $A^0_{\rm 4PN}$ is resummed using a (1,4) Padé approximant, i.e., $A^0(u;\nu) \equiv P^1_4[A^0_{\rm 4PN}(u;\nu)]$, with the logarithmic term treated as a constant in the Padé approximant. The tidal part of the interaction potential is known at next-to-next-to-leading order (NNLO, fractional 2PN) and reads $A^T(u) = -\sum_{\ell=2}^4 \kappa^T_\ell u^{2\ell+2}(1 + \bar{\alpha}_1^{(\ell)} u + \bar{\alpha}_2^{(\ell)} u^2)$, with only $\bar{\alpha}^{(2),(3)}_{1,2}$ known analytically [22]. For $\ell \geq 2$, the dimensionless tidal coupling constants are [20]

$$\kappa^T_\ell \equiv 2\left[\frac{1}{q}\left(\frac{X_A}{C_A}\right)^{2\ell+1} k^A_\ell + q\left(\frac{X_B}{C_B}\right)^{2\ell+1} k^B_\ell\right], \qquad (1)$$

where $q = M_A/M_B \geq 1$, $X_A \equiv M_A/M = q/(1+q)$, $X_B \equiv M_B/M = 1/(1+q)$, $k^{A,B}_\ell$, and $C_{A,B}$ are the dimensionless Love numbers and compactness of star A and B. All the information about the EOS is encoded in the κ^T_ℓ's. For typical compactnesses $C \sim 0.12$–0.2, $\kappa^T_2 \sim \mathcal{O}(10^2)$, and $\kappa^T_{3,4} \sim \mathcal{O}(10^3)$.

Stable circular orbits correspond to minima in u of $\hat{H}_{\rm eff}$ for a given value of p_φ. For any u, the condition $\hat{H}_{\rm eff}(u)' = 0$ yields $j^2(u) = -A'(u)/[u^2 A(u)]'$ for the angular momentum along circular orbits $j \equiv p_\varphi$ ($' \equiv \partial_u$). The orbital frequency reads $M\Omega(u;\nu) = \mu^{-1}\partial_j H_{\rm EOB} = j(u)A(u;\nu)u^2/(H_{\rm EOB}\hat{H}_{\rm eff})$. The end of the adiabatic (circular) dynamics is marked by the LSO, i.e., the inflection point of $\hat{H}_{\rm eff}$ that yields ($u_{\rm LSO}$, $j_{\rm LSO}$) and in turn the LSO orbital frequency $M\Omega_{\rm LSO}(\nu)$. The Schwarzschild LSO frequency is recovered by construction $M\Omega_{\rm LSO}(\nu = 0) = M\Omega^{\rm Schw}_{\rm LSO}$. The ν-dependent, nontidal, corrections to A are globally repulsive, i.e., $M\Omega_{\rm LSO}(\nu) > M\Omega^{\rm Schw}_{\rm LSO}$ [14]. The tidal contribution A^T is, instead, always attractive and moves $M\Omega_{\rm LSO}$ to lower frequencies. The LSO frequency results then as a balance between repulsive and attractive effects.

Spin effects are included following Ref. [17], which is robust enough for BNS realistic spin values (dimensionless magnitude $\chi_{A,B} \lesssim 0.1$). The spin-orbit interaction is taken at NNLO [23], the spin-spin interaction at leading order [24]. The spin gauge freedom is fixed according to Refs. [23,25]. To have circular orbits, we only consider spins parallel (or antiparallel) to the orbital angular momentum. The LSO computation is analogous to the nonspinning case. $M\Omega_{\rm LSO}$ is larger (smaller) than the nonspinning case for parallel (antiparallel) spins; i.e., the system is less (more) bound [13,17].

The complete nonadiabatic EOB model ($\mathcal{F}_\varphi \neq 0$) allows one to go beyond the adiabatic-circular-LSO analysis and to examine the model quantitatively with NR data. For the radiation reaction $\mathcal{F}_\varphi$ we use the tidal extension of the point-mass prescriptions of Ref. [4] and also include a radial component [26]. The point-mass dynamics is taken at 4PN in both the $A(u;\nu)$ and $\bar{D}^0(u;\nu) \equiv [A(u;\nu)B(u;\nu)]^{-1}$ functions, using in the latter the linear-in-ν 4PN coefficient obtained numerically [27,28]. Note that the formal regime of validity of the model may break when the dynamics is evaluated for $u \gtrsim u_{\rm LSO}$ since the two stars may be already in contact at those radial separations [20].

κ^T_ℓ universal relations.—We studied the dependence of $2M\Omega_{\rm LSO}$ and the binding energy per reduced mass at LSO, $E_{b\,\rm LSO} = (H_{\rm EOB} - M)/\mu$, when varying EOS, compactness, mass ratio, and spin. For each EOS in a sample of 12 realistic ones, we vary the mass of each star between $1.3M_\odot$ and the maximum mass allowed $M_{\rm max} \gtrsim 2M_\odot$. We found that both $2M\Omega_{\rm LSO}$ and $E_{b\,\rm LSO}$ are essentially independent of the choice of EOS when expressed versus any of the tidal coupling constants κ^T_ℓ. For example, Fig. 1 displays $2M\Omega_{\rm LSO}$ and $E_{b\,\rm LSO}$ versus the dominant coupling constant κ^T_2 for $q = 1$ and no spins. From the residuals (bottom panels), one sees that deviations from universality are below 0.2%. The same quasiuniversal behavior is also found for unequal mass, spinning BNS. Varying $1 \leq q \leq 2$ does not lead to curves significantly different from those in Fig. 1, the only difference being a narrower interval of variability of κ^T_2. By contrast, the spin-orbit coupling significantly changes the EOB LSO frequency and binding energy already at spin magnitudes $\chi \sim 0.01$–0.1. An example is given by Fig. 2, restricted to EOS ENG for clarity. The dimensionless spin value is chosen to be $\chi = \pm 0.1$.

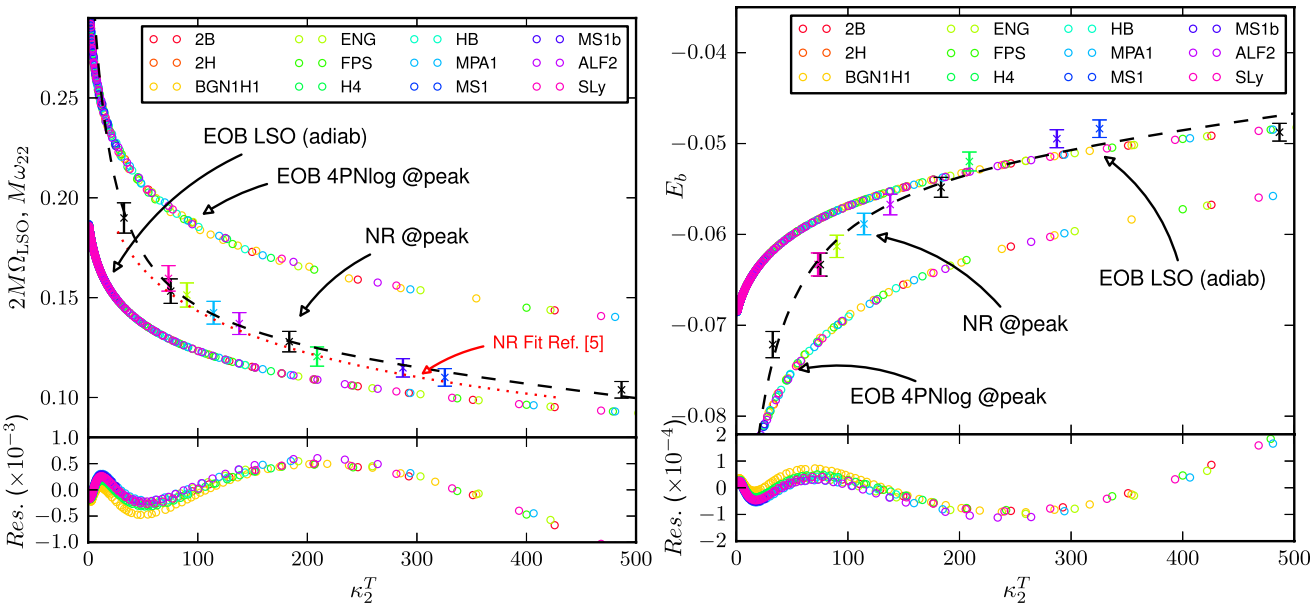

FIG. 1 (color online). GW frequency (left) and binding energy (right) versus the coupling constant κ_2^T for equal masses, irrotational mergers. Main panels: Circles refer to EOB quantities computed at either the adiabatic LSO ($2M\Omega_{\rm LSO}$, $E_{b\,\rm LSO}$) or the moment of merger ($M\omega_{22\,\rm mrg}^{\rm EOB}$, $E_{b\,\rm mrg}^{\rm EOB}$). Different colors refer to different EOS; crosses (with error bars) refer to NR quantities at the moment of merger ($M\omega_{22\,\rm mrg}^{\rm NR}$, $E_{b\,\rm mrg}^{\rm NR}$). Among these, the black crosses refer to polytropic EOS. The dashed black lines are the fits given in the text. The dotted red line in the left panel is the phenomenological fit of Ref. [5]. Bottom panels: Differences in $2M\Omega_{\rm LSO}$ and $E_{b\,\rm LSO}$ with respect to the fits of the LSO data. An analogue result holds for the nonadiabatic EOB quantities at the moment of merger. The EOS dependence is negligible: all quantities (EOB LSO, 4PNlog EOB, and NR) show κ_ℓ^T universality.

The difference between $q = 2$ and $q = 1$ curves is $\lesssim 0.5\%$. The spin dependence is linear for spins $\chi \lesssim 0.1$, as expected for the spin-orbit interaction. Note that the functional dependence $2M\Omega_{\rm LSO}(\kappa_2^T)$ [and similarly $E_{b\,\rm LSO}(\kappa_2^T)$] is algebraically complicated already for the simplest choice of the $A(u)$ function and cannot be made explicit. Both quantities can be robustly fitted to a low-order rational polynomial of the form $f(\kappa) = f(0)(1 + n_1\kappa + n_2\kappa^2)/(1 + d_1\kappa + d_2\kappa^2)$, where $f(0)$ is the point-mass LSO value $[2M\Omega_{\rm LSO}(0), E_{b\,\rm LSO}(0)] \approx (0.1892, -0.0688)$.

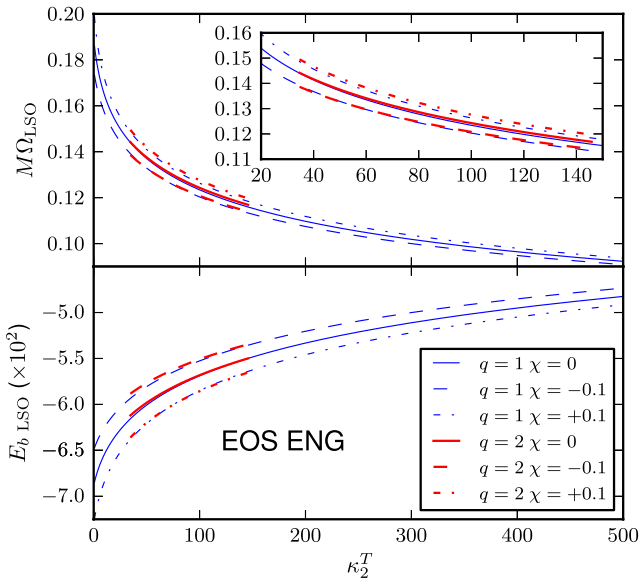

FIG. 2 (color online). GW frequency (top) and binding energy (bottom) versus the coupling constant κ_2^T at EOB LSO: varying mass ratio and spin magnitude. Only the ENG EOS is plotted for simplicity. The effect of mass ratio is almost negligible. The effect of spin is dominated by spin-orbit coupling.

As merger is approached, the dynamics enters a tidally dominated regime: the values of $2M\Omega_{\rm LSO}$ and $E_{b\,\rm LSO}$ are strongly influenced by tidal effects. Close to the LSO, the tidal potential $A^T(u;\nu)$ may become comparable or larger than $\nu\hat{a}(u;\nu) \equiv A^0(u;\nu) - (1 - 2u)$, which determines point-mass (ν-dependent) effects. One can see this in comparing the various contributions to the "radial force" $dA/dr = -u^2[-2 + \nu\hat{a}'(u;\nu) + A_T'(u;\nu)]$. For example, at LSO (EOS SLy, $\nu = 1/4$) one has for $C = 0.14$ and $\kappa_2^T = 274.51$, $u_{\rm LSO} \approx 0.1366$, which yield $\nu\hat{a}'(u) \approx 0.0703$ and $A_T'(u;\nu) \approx -0.1168$; for $C = 0.18$ and $\kappa_2^T = 58.52$, $u_{\rm LSO} \approx 0.1645$, which yield $\nu\hat{a}'(u) \approx 0.1127$ and $A_T'(u;\nu) \approx -0.0669$. Concerning the LSO frequency, one gets $M\Omega_{\rm LSO} = 0.0517$ for $C = 0.14$ and $M\Omega_{\rm LSO} = 0.06674$ for $C = 0.18$ [29]. The values of $M\Omega_{\rm LSO}$ and $E_{b\,\rm LSO}$ are rather close to the Schwarzschild ones, being the latter determined by $A(u;\nu = 0) = 1 - 2u$. The behavior is *not* a property of the LSO, but it is expected to hold also for $u > u_{\rm LSO}$, since $A^T(u) \propto u^6$; i.e., it holds during the whole merger process. By contrast, the universal curves extracted at separations larger than the LSO progressively flatten (the κ_ℓ^T dependency weakens) and

approach the degenerate point-mass case as the tidal interaction becomes negligible.

The complete nonadiabatic EOB dynamics can be continued also after the LSO crossing and the orbital frequency $M\Omega(t)$ develops a local maximum [12], likewise, the point-mass case. The analytical time-domain $\ell = m = 2$ EOB waveform is characterized by a peak in the modulus and a peak in the frequency $M\omega_{22}^{\rm EOB}$, reproducing the well-known qualitative structure of the NR waveforms, e.g., see Refs. [5,30]. In this sense, the complete tidal EOB waveform qualitatively implements "the merger" already at the analytical level, i.e., without NR tuning. We define the *moment of merger* (in both EOB and NR) as the peak of the amplitude of the $\ell = m = 2$ mode of the GW. This is an idealization since the actual merger process takes place during the last few orbits of the coalescence. As shown in Fig. 1, the EOB wave frequency $M\omega_{22\,\rm mrg}^{\rm EOB}$ and the binding energy $E_{b\,\rm mrg}^{\rm EOB}$ at the moment of merger are also characterized by a κ_ℓ^T universality.

Comparison with NR.—The adiabatic tidal EOB analysis captures the relevant qualitative features of the merger dynamics. Specifically, the quasiuniversal properties of $M\Omega$ and E_b close to the EOB LSO hold also for the actual NR merger frequency and binding energy. We stress that we do *not* advocate a formal link between the EOB LSO and NR quantities, but rather give a suggestive argument for the existence of these universal structures.

We performed new NR simulations of coalescing BNS, employing the BAM code and the method described in Refs. [30,31], though. (i) We use the Z4c formulation of Einstein's equations [32], and (ii) GWs are extracted from an extended wave zone [33]. The binaries are equal-mass, irrotational configurations with different EOSs. A $\Gamma = 2$ polytropic EOS model is employed to simulate different compactnesses $C_A = C_B = (0.12, 0.14, 0.16, 0.18)$; EOSs MS1, MS1b, H4, ALF2, MPA1, ENG, and SLy are employed for simulations with fixed isolation mass $M = 2 \times 1.35 M_\odot$. The evolutions cover about 10 orbits up to merger. These are among the longest BNS simulations ever performed and some of the few where an error analysis is available [8,12]. For each NR data set, we compute the binding energy per reduced mass $E_b^{\rm NR}$, subtracting the GW energy loss from the initial ADM mass, following Refs. [10,12,13]. Here, different from previous works, all the multipoles are included. GW frequency and binding energy are extracted at the moment of merger. We estimate error bars due to truncation errors and waveform finite extraction uncertainties from resolution tests for fewer configurations. More details on these simulations will be given elsewhere.

Recently, the authors of Ref. [5] proposed a phenomenological linear relation between the log of $M\omega_{22\,\rm mrg}^{\rm NR}$ and the quantity $\Lambda^{1/5} = (\frac{2}{3}k_2)^{1/5} C^{-1} = [(16/3)\kappa_2^T(q=1)]^{1/5}$ inspecting an independent sample of equal-mass, irrotational NR waveforms for six different EOSs. We believe the effectiveness of that empirical fit is explained by the κ_ℓ^T universality.

The NR GW frequency $M\omega_{22\,\rm mrg}^{\rm NR}$ and binding energy $E_{b\,\rm mrg}^{\rm NR}$ at the moment of merger are plotted as functions of κ_2^T in Fig. 1. The fit of Ref. [5] complements our numerical data, with which is perfectly consistent. As indicated by the figure, the NR points are compatible with the κ_ℓ^T universality. Similar to the EOB quantities, the NR data can be fitted to rational polynomials. We constrain the fit to the "black-hole limit" by factoring out the values $E_{b\,\rm mrg}^{\rm NR}(\kappa_\ell^T = 0) \approx -0.120$ and $M\omega_{22\,\rm mrg}^{\rm NR}(\kappa_\ell^T = 0) \approx 0.360$ as given by equal-mass binary black hole simulations [10]. The fitting function is $f(\kappa) = f(0)(1 + n_1\kappa + n_2\kappa^2)/(1 + d_1\kappa)$, with $(n_1, n_2, d_1) = (2.59 \times 10^{-2}, -1.28 \times 10^{-5}, 7.49 \times 10^{-2})$ for the frequency and $(n_1, n_2, d_1) = (2.62 \times 10^{-2}, -6.32 \times 10^{-6}, 6.18 \times 10^{-2})$ for the binding energy. Considering $E_b(\kappa)$ and $M\omega_{22}(\kappa)$ as a parametric curve, one obtains a relation between the binding energy and the frequency at the moment of merger that is essentially linear,

$$E_{b\,\rm mrg}^{\rm NR} \approx -0.284 M\omega_{22\,\rm mrg}^{\rm NR} - 0.0182, \tag{2}$$

with $M\omega_{22\,\rm mrg}^{\rm NR} \in [0.1, 0.360]$. Also, in this case the black hole limit is incorporated in the fit. Quantitatively, there are differences between the NR merger quantities ($M\omega_{22\,\rm mrg}^{\rm NR}$, $E_{b\,\rm mrg}^{\rm NR}$) and the corresponding EOB ones ($M\omega_{22\,\rm mrg}^{\rm EOB}$, $E_{b\,\rm mrg}^{\rm EOB}$); see Fig. 1. The relative difference on the relevant interval $\kappa_2^T \in [50, 350]$ is between 20–30% for the frequency and 10–20% for the binding energy. This quantitative disagreement is not surprising: hydrodynamics effects and nonlinear tidal interactions are not modeled in $A^T(u)$. At an effective level, the (uncalibrated) EOB 4PN tidal dynamics basically underestimates attractive effects and gives a larger (smaller) frequency (binding energy) at merger. Coincidentally, the adiabatic EOB LSO gives a rather good numerical approximation, especially for $\kappa_2^T \gtrsim 200$. The key, remarkable point here is that the adiabatic model already captures the κ_ℓ^T universality, indicating that the latter emerges fundamentally from the conservative dynamics. Furthermore, the simple LSO analysis gives reasonable estimates of merger relations for any EOS, mass ratio, and (aligned) spins.

Outlook.—Modeling GWs from neutron star mergers is a challenging open problem (see e.g., Ref. [34] for very recent work) that can be tackled interfacing accurate nonlinear simulations with the EOB analytical framework. While pursuing this approach we have identified κ_ℓ^T values as fundamental "coupling constants" of the binary tidal interactions, together with κ^T universal relations and their physical origin. An extension of the present work would be more multiorbit and precise NR simulation including, in particular, spins [13]. Future work will be devoted to exploring effective extensions of the nonadiabatic EOB model, e.g., the use of flexibility parameters or different

resummations of A^T [22]. Ultimately, a NR-tuned tidal EOB model is expected to deliver accurate merger waveforms for BNS GW detection, similar to the black hole binary case [11,19].

The κ^T universality has consequences for GW astronomy. For example, using EOB-based merger templates (containing the characteristic peak) in match filtered searches one might be able to accurately extract the value of κ_2^T from the template's peak [4]. A single measure of the frequency at the moment of merger would, thus, constrain both the EOS and the binding energy. The actual possibility to pursue this strategy deserves a study on its own. In this respect, the κ^T universality characterizing the merger has similarities with the findings of Ref. [35] and with the universal relations found for single neutron star properties [36]. Also, we propose to use the value of the merger frequency, as given by our fits, to mark the end of inspiral templates; this will improve the simple Schwarzschild LSO criterion, e.g., Ref. [6].

Interestingly, due to the coincidental "compensation" of finite mass effects in the tidally dominated regime, the Schwarzschild LSO values give very good estimates to the GW frequency and binding energy at BNS merger for irrotational binaries with $\kappa_2^T \sim 200$.

We thank B. Brügmann, T. Damour, and C. Van den Broeck for useful comments. This work was supported in part by DFG Grant SFB/Transregio 7 "Gravitational Wave Astronomy" and the Graduiertenakademie Jena. S. B. and Si. B. thank IHES for hospitality during the development of part of this work. Si. B. is supported by the Swiss National Science Foundation. M. U. is supported by CAPES under BEX 10208/12-7 and thanks TPI Jena for hospitality during the development of this work. Simulation were performed on the LRZ cluster in Münich.

[1] J. Abadie *et al.* (LIGO Scientific Collaboration, Virgo Collaboration), *Classical Quantum Gravity* 27, 173001 (2010).
[2] J. Aasi *et al.* (LIGO Scientific Collaboration, Virgo Collaboration), arXiv:1304.0670.
[3] J. S. Read, C. Markakis, M. Shibata, K. Uryu, J. Creighton, and J. Friedman, Phys. Rev. D **79**, 124033 (2009).
[4] T. Damour, A. Nagar, and L. Villain, Phys. Rev. D **85**, 123007 (2012).
[5] J. S. Read, L. Baiotti, J. D. E. Creighton, J. L. Friedman, B. Giacomazzo, K. Kyutoku, C. Markakis, L. Rezzolla, M. Shibata, and K. Taniguchi, Phys. Rev. D **88**, 044042 (2013).
[6] W. Del Pozzo, T. G. F. Li, M. Agathos, C. Van Den Broeck, and S. Vitale, Phys. Rev. Lett. **111**, 071101 (2013).
[7] L. Baiotti, T. Damour, B. Giacomazzo, A. Nagar, and L. Rezzolla, Phys. Rev. Lett. **105**, 261101 (2010).
[8] S. Bernuzzi, M. Thierfelder, and B. Brügmann, Phys. Rev. D **85**, 104030 (2012).
[9] K. Hotokezaka, K. Kyutoku, and M. Shibata, Phys. Rev. D **87**, 044001 (2013).
[10] T. Damour, A. Nagar, D. Pollney, and C. Reisswig, Phys. Rev. Lett. **108**, 131101 (2012).
[11] A. Taracchini, A. Buonanno, Y. Pan, T. Hinderer, M. Boyle *et al.*, Phys. Rev. D **89**, 061502 (2014).
[12] S. Bernuzzi, A. Nagar, M. Thierfelder, and B. Brügmann, Phys. Rev. D **86**, 044030 (2012).
[13] S. Bernuzzi, T. Dietrich, W. Tichy, and B. Bruegmann, arXiv:1311.4443 [Phys. Rev. D (in preparation)].
[14] A. Buonanno and T. Damour, Phys. Rev. D **59**, 084006 (1999).
[15] A. Buonanno and T. Damour, Phys. Rev. D **62**, 064015 (2000).
[16] T. Damour, P. Jaranowski, and G. Schäfer, Phys. Rev. D **62**, 084011 (2000).
[17] T. Damour, Phys. Rev. D **64**, 124013 (2001).
[18] L. Blanchet, Living Rev. Relativity **9**, 4 (2006).
[19] T. Damour, A. Nagar, and S. Bernuzzi, Phys. Rev. D **87**, 084035 (2013).
[20] T. Damour and A. Nagar, Phys. Rev. D **81**, 084016 (2010).
[21] D. Bini and T. Damour, Phys. Rev. D **87**, 121501 (2013).
[22] D. Bini, T. Damour, and G. Faye, Phys. Rev. D **85**, 124034 (2012).
[23] A. Nagar, Phys. Rev. D **84**, 084028 (2011).
[24] S. Balmelli and P. Jetzer, Phys. Rev. D **87**, 124036 (2013).
[25] T. Damour, P. Jaranowski, and G. Schäfer, Phys. Rev. D **78**, 024009 (2008).
[26] Contrarily to the case in Refs. [7,12], NR-determined next-to-quasi-circular corrections to the waveform and to $\mathcal{F}_\varphi$ are not included.
[27] L. Barack, T. Damour, and N. Sago, Phys. Rev. D **82**, 084036 (2010).
[28] E. Barausse, A. Buonanno, and A. Le Tiec, Phys. Rev. D **85**, 064010 (2012).
[29] We stress that the result is qualitatively and quantitatively robust when changing the PN order of A^0 from 3PN to the 5PN (the latter employs NR-tuned flexibility parameters [19]). We observe monotonic behavior with the various PN orders. The fractional difference between 5PN and 4PN is between 0.3% to 1% for $\kappa_2^T \gtrsim 50$ and up to 3% for $\kappa_2^T \in [10, 50]$.
[30] M. Thierfelder, S. Bernuzzi, and B. Brügmann, Phys. Rev. D **84**, 044012 (2011).
[31] B. Brügmann, J. A. Gonzalez, M. Hannam, S. Husa, U. Sperhake, and W. Tichy, Phys. Rev. D **77**, 024027 (2008).
[32] S. Bernuzzi and D. Hilditch, Phys. Rev. D **81**, 084003 (2010).
[33] D. Hilditch, S. Bernuzzi, M. Thierfelder, Z. Cao, W. Tichy, and B. Brügmann, Phys. Rev. D **88**, 084057 (2013).
[34] L. Wade, J. D. E. Creighton, E. Ochsner, B. D. Lackey, B. F. Farr *et al.*, arXiv:1402.5156.
[35] A. Bauswein and H.-T. Janka, Phys. Rev. Lett. **108**, 011101 (2012).
[36] K. Yagi and N. Yunes, Science **341**, 365 (2013).